This is an Accepted Manuscript of an article published by Taylor & Francis in Annals of the American Association of Geographers on 4 Apr 2022 (Published online), available online: http://www.tandfonline.com/10.1080/24694452.2022.2029342.

Association between global air pollution and COVID-19 mortality, a study of forty-six cities in the world

Yuan Meng [a], Man Sing Wong [a,b]*, Mei-Po Kwan [c,d] and Rui Zhu [a]

[a] Department of Land Surveying and Geo-Informatics, The Hong Kong Polytechnic University, Hong Kong; [b] Research Institute for Sustainable Urban Development, The Hong Kong Polytechnic University, Hong Kong; [c] Department of Geography and Resource Management, and Institute of Space and Earth Information Science, The Chinese University of Hong Kong, Hong Kong; [d] Department of Human Geography and Spatial Planning, Utrecht University, 3584 CB Utrecht, The Netherlands

* Correspondence: Ls.charles@polyu.edu.hk; Tel.: +852-3400-8959

Association between global air pollution and COVID-19 mortality, a study of forty-six cities in the world

The ambient air pollution plays a significant role in an increased risk of incidence and mortality of the coronavirus disease 2019 (COVID-19) on a global scale. This study aims to understand the multi-scale spatial effect of the global air pollution on the COVID-19 mortality. Based on 46 cities from six countries worldwide between 1 Apr. 2020 and 31 Dec. 2020, a Bayesian space-time hierarchical model (BSTHM) was utilized based on the lag effects of 7, 14 and 21 days to quantify the relative risks of NO_2 and $PM_{2.5}$ on the daily deaths of COVD-19, accounting for the effect of meteorological and human mobility variability based on global and city level. Results show that positive correlations between air pollution and COVID-19 mortality are observed, with the relative risks of NO_2 and $PM_{2.5}$ ranging from 1.006 to 1.014 and from 1.002 to 1.004 with the lag effects of 7, 14 and 21 days. For the individual-city analysis, however, both positive and negative associations are found between air pollution and daily mortality, showing the relative risks of NO_2 and $PM_{2.5}$ are between 0.754 and 1.245, and between 0.888 and 1.032, respectively. The discrepancies of air pollution risks among cities were demonstrated in this study, and further allude the necessity to explore the uncertainty in the multi-scale air pollution – mortality relationship.

Keywords: COVID-19; air pollution; Bayesian space-time hierarchical model; multi-scale analysis

Introduction

The exposure to air pollution has been widely recognized to have a substantial impact on human health, including respiratory and cardiovascular disease (Brunekreef and Holgate 2002; Lelieveld et al. 2015). The rapid urbanization processes comprises various of air pollution, i.e. industrial air pollution from fossil fuel combustion, emissions from biomass burning such as nitrogen dioxide (NO_2), and fine particulate matter with a diameter less than 2.5 μm ($PM_{2.5}$) (Akimoto 2003; He, Huo, and Zhang 2002). Study has projected a 50% increase in mortality corresponding to the ambient air pollution by 2050 (Lelieveld et al. 2015), revealing the necessity of intensive air quality control measures on a global scale.

With the rapid emergence of the coronavirus disease 2019 (COVID-19), the government-enforced policies, including lockdowns and social-distancing measures, have drastically decrease socioeconomic activities and led to significant air pollution changes (Giani et al. 2020; He, Pan, and Tanaka 2020). Existing study has provided evidence that the lockdowns have caused 60% and 31% decline in NO_2 and $PM_{2.5}$ and an increase trend in O_3 until 15 May 2020 in 34 countries (Venter et al. 2020). It provides an unprecedented opportunity to estimate the impact of air pollution counterfactual to business-as-usual situations on the respiratory disease, i.e. COVID-19, on a global scale.

Among various air pollutants, NO_2 and $PM_{2.5}$, the major pollutants of anthropogenic emission, have been studied with the potential risks on the incidence and mortality of COVID-19. Villeneuve and Goldberg (2020) evaluated both tropospheric and ground-level NO_2 and $PM_{2.5}$ with daily or annual mean values based on varied time lag effects in different regions. Ogen (2020) focused on the satellite-based NO_2 distribution and analyzed its association with the fatality of COVID-19 in France, Germany, Italy and Spain, and further indicates the close relationship between the long-term exposure to NO_2 and the COVID-19 fatality. A study on China based on two-week confirmed cases of COVID-19 suggests that a 10 $\mu g/m^3$ increase in NO_2 and $PM_{2.5}$ are associated with the 6.94% and 2.24% increases of the confirmed cases based on the lag effect of 0 – 14 (Zhu et al. 2020a). However, a study proposed by Gujral and Sinha (2021) shows negative association between ground-based $PM_{2.5}$ and the COVID-19 confirmed cases in Los Angeles, U.S., indicating the discrepancies of air pollution – COVID-19 incidences in different areas.

Other determinants of COVID-19 including meteorological and socioeconomic factors are required to be controlled when estimating the association of air pollution and COVID-19 incidence and mortality (Chowkwanyun and Reed Jr 2020; Yancy 2020; Sarkodie and Owusu 2020; Kwok et al. 2021). Xie and Zhu (2020) adopted 122 cities from China within one month and revealed a positive linear relationship between mean temperature and the number of the COVID-19 confirmed cases. In contrast, Shao, Xie, and Zhu (2021) suggested that on a global scale, ambient temperature is negatively associated with the COVID-19 transmission mediated by human mobilities. Meteorological factors also include humidity and wind speed, in which 1 unit increase of absolute humidity corresponds to the decreasing trend of COVID-19 mortality in Wuhan, China (Ma et al. 2020) while cities with low wind speed that is associated with atmospheric stability had higher numbers of COVID-19 incidence and mortality (Coccia 2021). Socioeconomic factors such as built environment and human mobilities have also been considered in the epidemiological modelling. Existing research has revealed that higher betweenness centrality of transport nodes and population density in the built-up regions are positively associated with COVID-19 infection ratios in China (Li, Ma, and Zhang 2021). Moreover, studies have estimated the COVID-19 infectious transmission by modelling human mobility patterns (Chang et al. 2021), and suggested the effectiveness of travel restrictions combined with transmission-reduction interventions on mitigating COVID-19 epidemic (Chinazzi et al. 2020).

Statistical models to estimate the association between air pollution and COVID-19 incidence and mortality vary among studies. Existing research has widely utilized Pearson correlation (Bashir et al. 2020), multiple linear regression (Andrée 2020; Coccia 2020; Barnett-Itzhaki and Levi 2021), difference-in-differences (DID) model (Ming et al. 2020; He, Pan, and Tanaka 2020), scenario analysis (Shan et al. 2020), generalized linear model (GLM) (Travaglio et al. 2021) and generalized additive model (GAM) (Prata, Rodrigues, and Bermejo 2020; Zhu et al. 2020b). As these models were proposed in different areas with varied time lag effect, model comparisons based on the same spatio-temporal scales are required to assess their accuracies.

Despite of the analysis on the different air pollution metric, additional determinants including meteorological and human mobility factors and varied statistical models that have been discussed, existing studies on the COVID-19 incidence and mortality mainly focused at city level and country level. Considering of the pandemic transmission trends among countries, it is necessary to study in a wider global perspective. Although several studies have investigated the global patterns of the air pollution and COVID-19 epidemic variation (Venter et al. 2020; Forster et al. 2020; Le Quéré et al. 2020), there lacks a deeper understanding of the impact of the global trending air pollution mediated by meteorological and human mobility patterns. Moreover, the influence of multi-scale spatial analysis should be considered to reduce the biases caused by constant spatial units. In addition, the performance of models that have been proposed in the association analysis needs to be evaluated to assure the model accuracies.

In this study, we focus on the association between air pollution and COVID-19 incidence in a global scale. Based on 46 cities from six countries between 1 Apr. 2020 and 31 Dec. 2020, a Bayesian space-time hierarchical model (BSTHM) was utilized to estimate the impact of ground-based air pollution including NO_2 and $PM_{2.5}$ on the COVID-19 mortality controlling by the variables of meteorological factors and human mobility frequencies. The relative risks of different air pollutants were estimated based on the overall global scale-and spatial multiscale-perspective. In addition, model comparison was proposed among GLM, GAM and BSTHM to evaluate the model effectiveness.

Materials and Methods

Study Area

Considering of the data availability, including the exposure to the air pollution and the corresponding COVID-19 deaths on a finer spatial level, about 46 cities from six countries that consists of high-quality air station data, COVID-19 mortality data and other controlling variable between 1 Apr. 2020 and 31 Dec. 2020 were selected for statistical analysis in the following section. As shown in Table 1, five cities from Canada, 1 city from Germany, 1 city from China, 2 cities from Mexico, 1 city from Netherlands, 36 cities/counties from U.S. were selected as the study areas.

Table 1. Selected countries and cities as study areas.

Countries	Cities/Counties
Canada	Edmonton, Calgary, Ottawa, Toronto, Montreal
Germany	Berlin
China	Hong Kong
Mexico	Guadalajara, Monterrey
Netherlands	Amsterdam
U.S.	Ada, Alameda, Bernalillo, Clark, Cook, Dallas, Denver, District of Columbia, Duval, El Paso, Franklin, Fresno, Fulton, Harris, Hartford, Henrico, Hinds, King, Los Angeles, Maricopa, Marion, Milwaukee, Multnomah, New York City, Oklahoma, Philadelphia, Pima, Providence, Ramsey, Salt Lake, San Diego, San Francisco, Santa Clara, Suffolk, Wake, Wayne

Air Pollution and Meteorological Data

Although satellite data such as TROPOspheric Monitoring Instrument (TROPOMI) in

Sentinel-5 Precursor satellite shows the potential to monitor spatio-temporal air pollution distribution in a global scale, the column concentration obtained from the satellite data cannot efficiently represent ground-level air pollutants. To fill this gap, this study adopted station-based air pollution and meteorological data from the Air Quality Open Data Platform (see https://aqicn.org/data-platform/covid19/). Specifically, daily air pollutants including NO_2 and $PM_{2.5}$, and daily meteorological data including daily humidity, pressure, temperature and wind speed between 1 Apr. 2020 and 31 Dec. 2020 were collected from the selected cities. On this basis, missing values from the daily air pollution and meteorological data were further processed using the KalmanSmoother based on an autoregressive integrated moving average (ARIMA) model (Bishop and Welch 2001).

Mobility Data from Apple

Human mobilities play a significant role in estimating epidemic disease transmission. To analyze the effect of human mobility patterns in different regions, daily mobility data were collected from the Apple Mobility Trends Reports (see https://covid19.apple.com/mobility). Specifically, the data calculate the comparative trip patterns for the report date to the baseline day (13 Jan. 2020). The mobility data take 100 as the baseline, with the negative changes lower than 100 and the positive changes higher than 100. In this study, two types of transportation are considered, including driving and walking transportation. In addition, the missing values in the temporal mobility data were filled using the ARIMA model.

Other Data as Controlling Variables

Four datasets, including the accessibility to the healthcare, the global friction surface, The NOAA Climate Data Record (CDR) of AVHRR Normalized Difference Vegetation

Index (NDVI), and the nighttime data from the Visible Infrared Imaging Radiometer Suite (VIIRS) Day/Night Band (DNB) were adopted to distinguish additional physical and socioeconomic conditions among cities. In particular, the accessibility to the healthcare in the year 2019, which quantifies the land-based travel time to the nearest hospital or clinic, was averaged into city scale. The global friction surface in 2019, enumerating the travel speed for all land pixels, which is considered as the potential indicator for estimating COVID-19 transmission, was also averaged into city scale. Both the accessibility to the healthcare dataset and the global friction surface dataset were collected from the research proposed by Weiss et al. (2020). In addition, city-level averaged NDVI and DNB radiance values between 1 Apr. 2020 and 31 Dec. 2020 were calculated from the NOAA CDR of AVHRR NDVI and VIIRS/ DNB nighttime data, separately. In addition, the global population in 2019 were collected from the LandScan (see https://landscan.ornl.gov) as the offset variable in the statistical analysis in the following section.

COVID-19 Data

The COVID-19 mortality data from 46 cities between 1 Apr. 2020 and 31 Dec. 2020 were collected from multiple sources, which are displayed in Table 2. The daily deaths were calculated based on the total deaths provided in the COVID-19 data.

Table 2. Data sources of COVID-19 mortality in different countries.

Countries	Data sources
Canada	COVID-19 Canada Open Data Working Group (https://github.com/ccodwg/Covid19Canada)
Germany	Das Datenportal für Deutschland (https://www.govdata.de)
China	DATA.GOV.HK (https://data.gov.hk/en-data/dataset/hk-dh-chpsebcddr-novel-infectious-agent)

Mexico	Covid-19 México (https://datos.covid-19.conacyt.mx/#DownZCSV)
Netherlands	Dataregister van de Nederlandse Overheid (https://data.overheid.nl)
U.S.	The New York Times (https://github.com/nytimes/covid-19-data)

Statistical Models

The BSTHM, composed by the hierarchical Bayesian model and the space-time interaction model, consists of three components: the overall spatial, temporal and the space-time interaction. It has been commonly applied in many fields such as public health (Liao et al. 2016; Richardson, Abellan, and Best 2006; Knorr-Held 2000), population assessment (Wang et al. 2021) and air pollution modeling (Li et al. 2018a; Li et al. 2018b). Compared with other statistical models such as GLM and GAM, hierarchical Bayesian model accommodates unobserved values and prior probability distributions to improve estimation accuracies (Dunson 2001).

Specifically, we assume that y_{it} is the deaths in the city $i = (1,2,\ldots,N)$ at the time point $t = (1,2,\ldots,T)$, the number of daily deaths can be modeled by the Poisson regression with the log link function:

$$y_{it} \sim Poisson(n_i r_{it}) \qquad (1)$$

where n_i indicates the base distribution in the city i, and r_{it} represents the underlying mortality risk, which can be further modeled as follows:

$$\begin{aligned} \log(r_{it}) = \alpha + \theta_i + \delta_t + \gamma_{it} + \beta_{no2} x_{it,no2} + \beta_{pm25} x_{it,pm25} + \beta_{humi} x_{it,humi} \\ + \beta_{pres} x_{it,pres} + \beta_{temp} x_{it,temp} + \beta_{wind} x_{it,wind} + \beta_{driving} x_{it,driving} \\ + \beta_{walking} x_{it,walking} + \beta_{acce} x_{i,acce} + \beta_{fric} x_{i,fric} + \beta_{NDVI} x_{i,NDVI} \\ + \beta_{night} x_{i,night} + \log(x_{i,pop}) + \varepsilon_{it} \qquad (2) \end{aligned}$$

in which β_{no2}, β_{pm25}, β_{humi}, β_{pres}, β_{temp}, β_{wind}, $\beta_{driving}$, $\beta_{walking}$, β_{acce}, β_{fric}, β_{NDVI} and β_{night} refer to the regression coefficients of daily NO_2, $PM_{2.5}$, humidity, pressure, mean temperature, mean wind speed, and the daily trip based on the driving and walking transportation, accessibility to the healthcare, the degree of friction, NDVI and the DNB radiance values with the following prior distributions $\pi(\cdot)$ assigned to the coefficients:

$$\pi(\beta) = N(0{,}1000) \tag{3}$$

In addition, α indicates the sum of the intercept. θ_i, δ_t and γ_{it} refer to the spatial main effect, temporal main effect and the space-time interaction. $\log(x_{i,pop})$ represents the offset variable based on the total population in each region. ε_{it} is the additional residual term. Moreover, the 7, 14 and 21 day-lag effects of socioeconomic and environmental factors on COVDI-10 mortality are considered.

Prior distributions are further assigned to the parameters above. The Besag York Mollié (BYM) model is employed to the spatial main effect, temporal main effect θ_i and δ_t, in which the BYM model is a convolution of a spatially structured and spatially unstructured random effect (Besag, York, and Mollié 1991). Specifically, the spatial structure is applied by the conditional autoregressive (CAR) models. The prior of θ_i, δ_t and γ_{it} are modeled as follows:

$$\theta_i|\boldsymbol{\theta}_{-i}, \boldsymbol{W} \sim N\left(\frac{\rho_s \sum_{j=1}^{N} w_{ij}\theta_j}{\rho_s \sum_{j=1}^{N} w_{ij} + 1 - \rho_s}, \frac{\tau_s^2}{\rho_s \sum_{j=1}^{N} w_{ij} + 1 - \rho_s}\right) \tag{4}$$

$$\delta_t|\boldsymbol{\delta}_{-t}, \boldsymbol{D} \sim N\left(\frac{\rho_t \sum_{j=1}^{T} d_{ij}\delta_j}{\rho_t \sum_{j=1}^{T} d_{ij} + 1 - \rho_t}, \frac{\tau_t^2}{\rho_t \sum_{j=1}^{T} d_{ij} + 1 - \rho_t}\right) \tag{5}$$

$$\gamma_{it} \sim N(0, \tau_k^2) \tag{6}$$

where $\boldsymbol{W} = (w_{ij})$ and $\boldsymbol{D} = (d_{tj})$ represent the neighborhood matrix and the time adjacency, respectively, where $w_{ij} = 1$ and $d_{tj} = 1$ if areas (i, j) share a common border and time $|j-t|=1$; otherwise, $w_{ij}=0$ and $d_{tj}=0$. (ρ_s, ρ_t) and (τ_s, τ_t, τ_k) refer to the parameters of the fixed uniform and inverse-gamma distribution, respectively, the prior of which is modeled as:

$$\rho_s, \rho_t \sim \text{Uniform}(0,1) \quad (7)$$

$$\tau_s, \tau_t, \tau_k \sim \text{Inverse}-\text{Gamma}(1,0.01) \quad (8)$$

Specifically, the neighborhood matrix is constructed based on the spatial distribution among cities, with $w_{ij}=1$ among each pair of adjacent cities and $w_{ij}=0$ otherwise.

The proposed BSTHM was implemented Markov chain Monte Carlo (MCMC) method and Gibbs sampling. Air pollutants including daily NO_2, $PM_{2.5}$ are utilized for estimating the number of deaths while meteorological factors, human mobilities, population and other factors are considered as controlling variables. The collinearity of variables was assessed using the variance inflation factor (VIF). Then, the estimated relative risk (RR), which is proposed based on the exponential transformation of the modelling coefficients, were calculated to estimate the impact of air pollutants on the changes of COVID-19 mortality.

Results

Descriptive Analysis

Table 3 shows the statistics of the daily deaths of COVID-19, air pollutants, meteorological factors, human mobility, population and other controlling variables in each city. Daily deaths vary from 0 to 1221, and daily NO_2 and $PM_{2.5}$ are 7.186 ppb and 33.783 $\mu g/m^3$, respectively. The mean daily humidity, pressure, temperature and the wind speed are 62.708 percent, 1011.274 mb, 17.018 °C and 2.687 m/s. For the urban mobility, the daily changes of driving and walking transportation are 103.482 and 110.176, respectively. In addition, the average values of accessibility to healthcare, the degree of friction, NDVI and nighttime radiance are 12.191, 0.004, 1652.558 and 18.484, respectively.

Table 3. Summary of the ground station data, meteorological data, mobility data, other controlling variables, and the COVID-19 mortality.

Variables	Daily measures				
	Min.	Max.	Mean	Std. Dev.	Var.
Daily deaths	0	1221	7.63	33.481	1120.971
Air pollutant					
NO_2 (ppb)	0.100	49.100	7.186	5.324	28.349
$PM_{2.5}$ ($\mu g/m^3$)	0.000	404.000	33.783	21.117	445.942
Meteorological factors					
Humidity (percent)	0.000	100.000	62.708	21.740	472.630
Pressure (mb)	415.400	1039.500	1011.274	26.257	689.446
Temperature (℃)	-17.700	39.200	17.018	8.710	75.867
Wind speed (m/s)	0.034	17.000	2.687	1.630	2.657
Human mobility					
Driving	22.390	209.340	103.482	30.682	941.367
Walking	7.870	295.690	110.176	45.153	2038.763
Population	2.471E+05	1.008E+07	2.037E+06	2.041E+06	4.164E+12
Other controlling variables					
Accessibility to healthcare	1.597	47.056	12.191	11.282	127.274
Friction	0.001	0.013	0.004	0.003	0.000
NDVI	953.004	2435.288	1652.558	399.947	159957.745
Nighttime radiance	1.136	49.768	18.484	13.317	177.333

Overall BSTHM Results

Fig. 1 shows the relative risk with 95% credible interval of air pollutants on the COVID-19 mortality with time lag 7, lag 14 and lag 21. In summary, the increasing values of NO_2 and $PM_{2.5}$ are positively correlated with COVID-19 mortality, indicating increasing daily deaths with higher NO_2 and $PM_{2.5}$ exposure. It is reasonable that both NO_2 and $PM_{2.5}$ and COVID-19 mortality have positive association since the decreasing of NO_2 and $PM_{2.5}$ could reduce the respiratory mortality has been demonstrated in other studies (Liu et al. 2019; Di et al. 2017; Khomenko et al. 2021). In addition, the association between NO_2, $PM_{2.5}$ and COVID-19 mortality vary according to the different time lag effects.

In particular, the relative risk of 1 ppb increase in NO_2 with 7 days lag effect is 1.009 (Confidence Interval (CI): 1.003 to 1.014). For the lag effect of 14 days, the relative risk of 1.014 is revealed with the confidence interval between 1.014 and 1.02, which is approximately 0.5% higher than the relative risk based on 7 days lag effect. Meanwhile, the relative risk of NO_2 with 21 days lag effect is 1.006 (CI: 0.999 to 1.012), which is 0.3% and 0.8% lower than those of 7 days and 21 days lag effects. For the relative risk of $PM_{2.5}$, similar patterns are revealed with the lag effects of 7 days and 14 days, representing approximately 0.2% increase (CI: 1.001 to 1.003) in daily death with 1 $\mu g/m^3$ increase in $PM_{2.5}$. Changes are revealed in the lag effect of 21 days, showing the relative risk of 1.004 with the confidence interval between 1.002 and 1.006, revealing approximately 0.2% higher than the relative risks based on 7-and 14-day lag effects.

Despite the varied lag effects (the association analysis without time lag effects is excluded considering the incubation period of COVID-19), the results indicate that higher exposures to NO_2 and $PM_{2.5}$ are estimated to increase the risks of COVID-19 mortality from the perspective of global cities. Because this study was conducted between 1 Apr. 2020 and 31 Dec. 2020, the potential influence of lockdown and restricted social distancing policies were concerned, measured by human mobility data. On the other hand, as the public vaccination started at the end of 2020 (Mathieu et al.

2021), its impacts on COVID-19 mortality are not discussed in this study. However, as the proposed controlling variables in BSTHM might not completely depict the environmental and socioeconomic conditions of individual cities, the discrepancies of relative risks among cities are not discussed. To fill this gap, the air pollution – mortality association analysis is proposed in the following section.

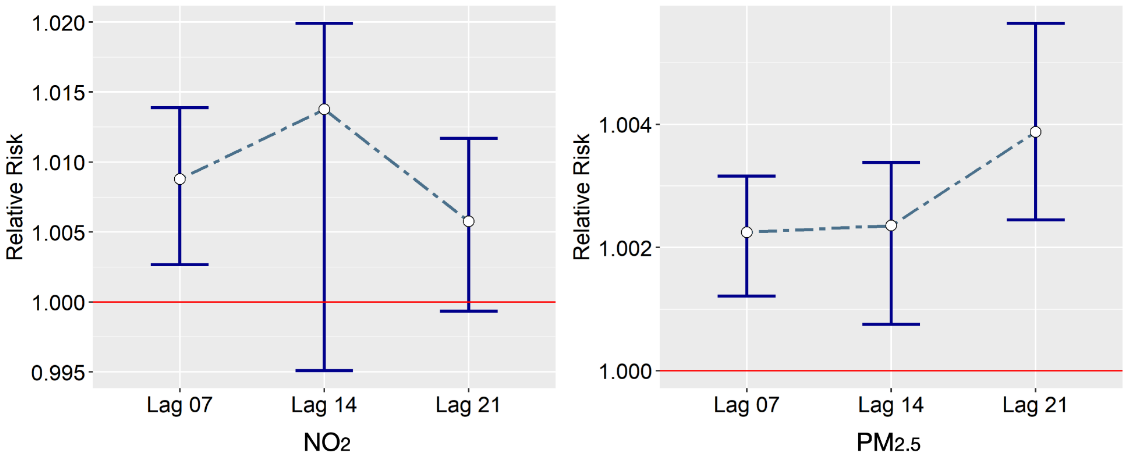

Fig. 1. Relative risk (with 95% credible interval) of air pollutants on the COVID-19 mortality with different time lag effects.

City-level Analysis

Changes of the study areas show significant impact on the air pollution - COVID-19 mortality analysis. After analyzing the overall impacts of NO_2 and $PM_{2.5}$ on COVID-19 mortality based on all the selected cities, we further focus on the relative risks of individual cities separately. The air pollution - COVID-19 mortality association of each city was estimated using Bayesian hierarchical modelling. As no spatial adjacency issue was found in individual cities, the spatial effect was removed from the proposed models.

Fig. 2 shows the relative risks of NO_2 with time lag effects of 7, 14 and 21 days of individual cities. In summary, the relative risks of NO_2 exposure vary among cities. Despite the different time lag effects, most of the cities show positive impact of NO_2 –

COVID-19 mortality association. It should be noted that significant discrepancies of relative risks are revealed among U.S. Henrico and other cities, showing large range confidence intervals based on all lag effects, with dramatically lower and higher relative risks based on 7 days and 14 days lag effects, respectively. No significant differences of relative risks are revealed among other cities for the lag effects of 7, 14 and 21 days, within the values between 0.948 and 1.138, between 0.973 and 1.152 as well as between 0.935 and 1.141. However, the results still revealed negative association between NO_2 and COVID-19 mortality in many cities, such as the relative risks based on 14- and 21-day lag effects in Hong Kong and 14-day lag affect-based relative risks in U.S. Suffolk and U.S. Wake. Further explanations about the negative trends are discussed later in this section.

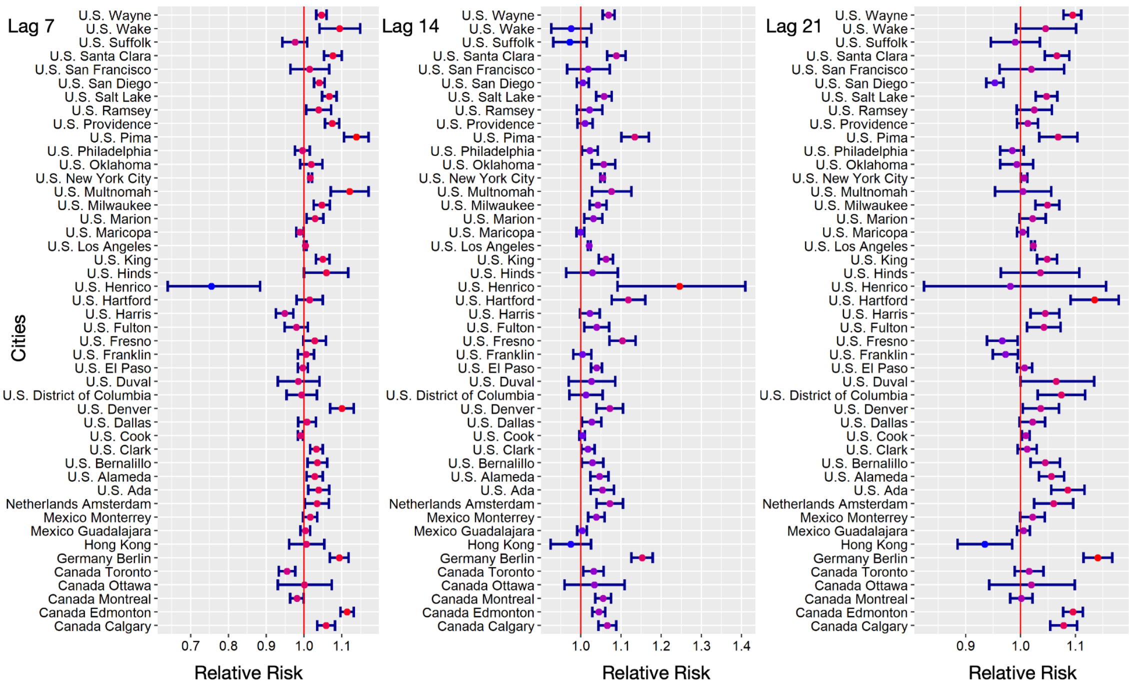

Fig. 2. Relative risk (with 95% credible interval) of NO_2 with time lag effects of 7, 14 and 21 days at the city scale.

The relative risks of $PM_{2.5}$ on the daily death of COVID-19 are shown in Fig. 3. The estimated relative risks based on 7-, 14- and 21-day effects range between 0.887

and 1.032, between 0.968 and 1.013, between 0.971 and 1.023. As with the relative risks of NO_2, no significant changes are shown in most of the cities. However, anomalies are observed, indicating significant discrepancies or negative trends, in several cities, such as the 7-day lag effect based relative risk in U.S. Providence, U.S. Pima, Canada Edmonton and Canada Calgary, 14-day lag effect based relative risk in Hong Kong, U.S. Pima, U.S. Henrico and U.S. Hartford, and 21-day lag effect based relative risk in Canada Calgary, Canada Edmonton, Hong Kong and U.S. Pima.

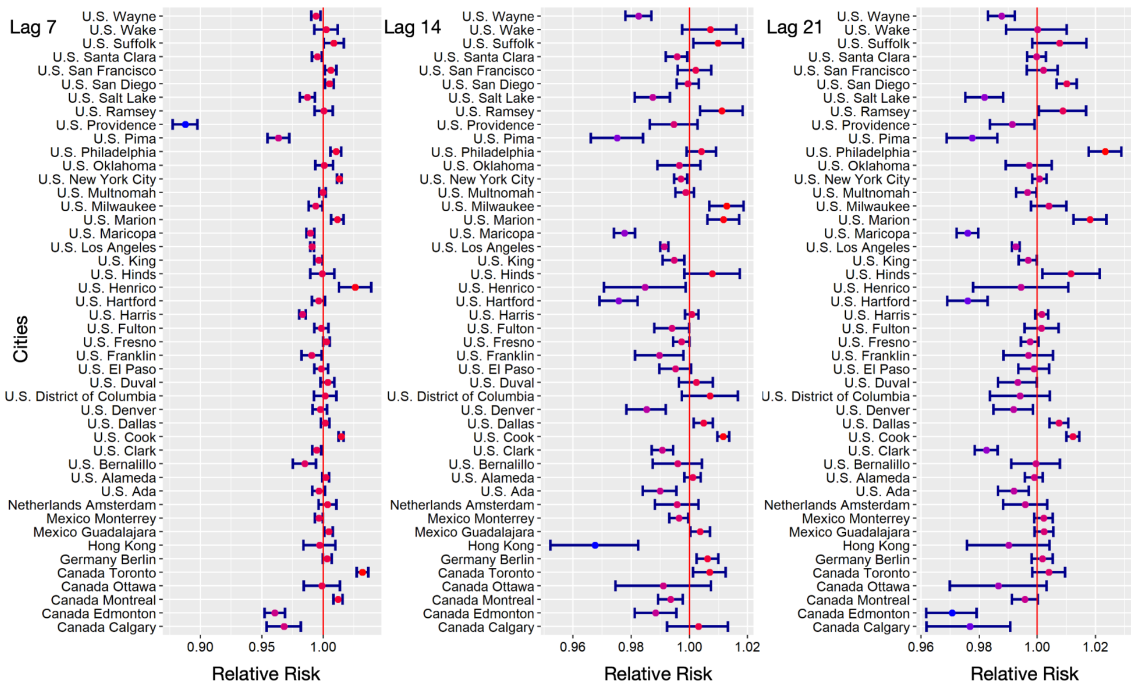

Fig. 3. Relative risk (with 95% credible interval) of $PM_{2.5}$ with time lag effects of 7, 14 and 21 days at the city scale.

The question of how to interpret these anomalies in the relative risks is important in the air pollution evaluation, especially the anthropogenic emissions. To solve this issue, deeper investigation on daily death, NO_2 and $PM_{2.5}$ emission as well as the human mobility for individual cities are proposed. As the number of deaths may influence the relative risk estimation (the smaller number of daily deaths, such as 0 death per day, could lead to estimation biases), the total deaths of COVID-19 during 1

Apr. 2020 to 31 Dec. 2020 in individual cities were calculated. As displayed in Fig. 4, small number of total deaths are found in cities such as Hong Kong, U.S. Hinds, U.S. Henrico, Canada Calgary, Canada Ottawa, U.S. Multnomah and U.S. Salt Lake, with the total number of deaths lower than 600. It is consistent with the relative risk biases that the impacts of NO_2 are dramatically lower and higher with 7- and 14-day lag effect with large range of confidence intervals in U.S. Henrico, as well as the negative relative risk in U.S. Salt Lake. The small number of deaths also provide hints in evaluating the relative risk biases of $PM_{2.5}$, suggesting that the smaller number of deaths may cause the significant negative relative risks in Hong Kong, Canada Calgary, Canada Ottawa and U.S. Multnomah. In summary, the potential impact of air pollution could be estimated with significant biases faced with smaller number of daily deaths. However, there are also other potential factors that may influence the relative risk estimation.

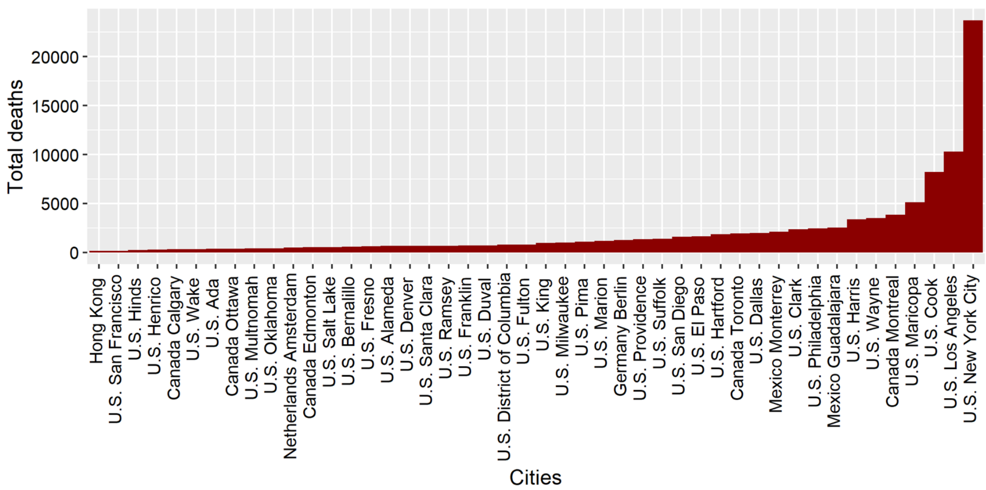

Fig. 4. Total deaths of COVID-19 during 1 Apr. 2020 to 31 Dec. 2020 in individual cities.

As with the small number of deaths, the level of air pollution plays a dominated role in evaluating the potential risks of air pollution in different cities (Chen et al. 2012). Fig. 5 displays the average daily emissions of NO_2 and $PM_{2.5}$ during 1 Apr. 2020 to 31 Dec. 2020 in each city. Several cities with lower levels of NO_2 and $PM_{2.5}$ reported anomalies in relative risks estimation. For example, Henrico in the U.S. with average daily NO_2 emissions lower than 2 ppb, shows significant negative trends in evaluating the relative risks of NO_2 on COVID-19 mortality. The lower emissions of $PM_{2.5}$ in Canada Calgary and Canada Edmonton, which are approximately 20 $\mu g/m^3$, also provide evidence on the biases of relative risk estimation. However, as lower-level air pollution may reduce the impact of NO_2 and $PM_{2.5}$ on mortality assessment, leading to biases in relative risk estimation, no evidence has been provided whether different air pollution levels are significantly correlated with the accuracies of potential risk estimation on cause-specific mortality.

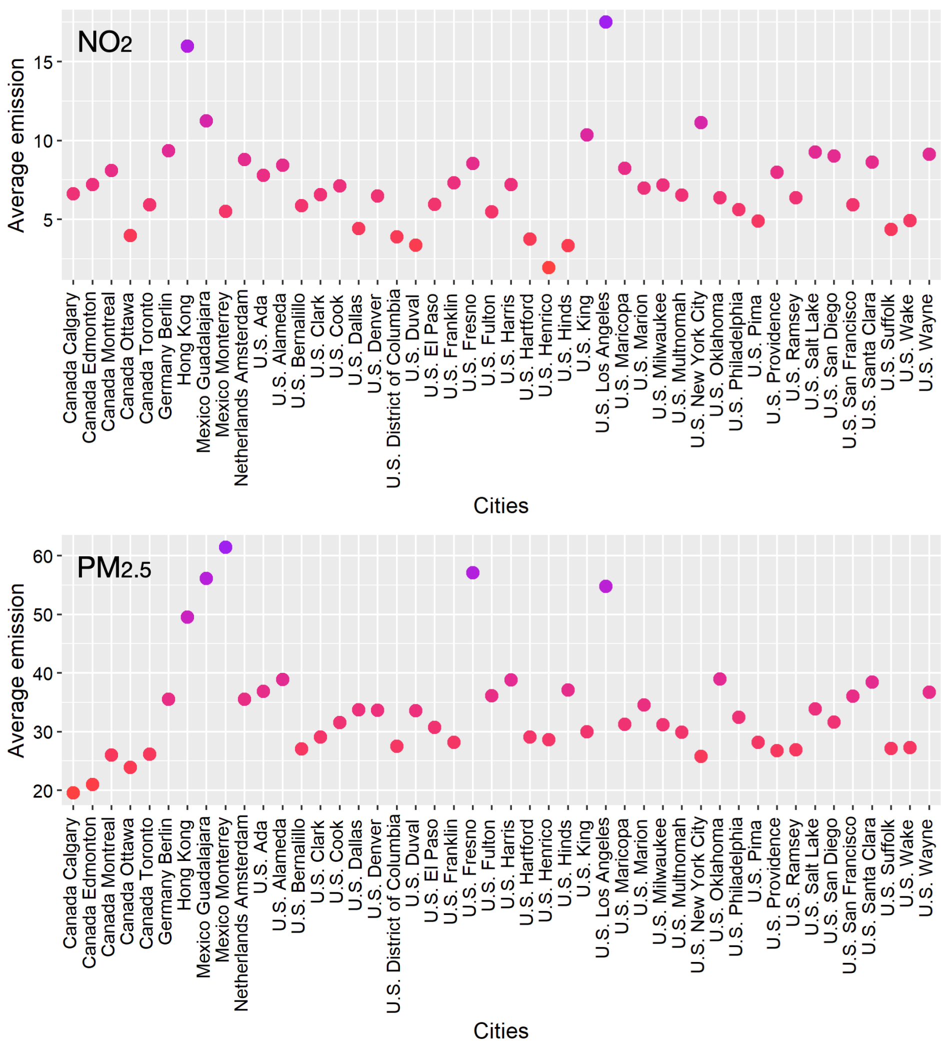

Fig. 5. Average air pollution emission during 1 Apr. 2020 to 31 Dec. 2020 of individual cities.

Our analysis has also considered the levels of human activity restriction to assess the role of anthropogenic emissions. Generally, the decrease of driving trips could reduce anthropogenic emissions (Meng et al. 2021), while the lower-level walking activities show the potential to reduce the risk of virus transmission (Chu et al. 2020). This study proposed a mobility variation index to measure the overall trends and changes of driving and walking transportation in each city using the Apple mobility data:

$$MV_i = \begin{cases} \sqrt{\dfrac{Mobility_{max,i} - \sum_{d=1}^{n} Mobility_{i,d}/n}{\left(\sum_{d=1}^{n} Mobility_{i,d}/n\right)^2}}, & \sum_{d=1}^{n} Mobility_{i,d} \geq 0 \\ -\sqrt{\dfrac{\left|Mobility_{min,i}\right| - \left|\sum_{d=1}^{n} Mobility_{i,d}/n\right|}{\left(\sum_{d=1}^{n} Mobility_{i,d}/n\right)^2}}, & \sum_{d=1}^{n} Mobility_{i,d} < 0 \end{cases} \quad (9)$$

where MV_i represents the quantified mobility variation of the *i*th city. $Mobility_{max,i}$ and $Mobility_{min,i}$ indicate the maximum and the minimum value of daily mobility changes, respectively, which are calculated from the daily mobility data represented by the Apple Mobility Trends Reports. As the mobility data take 100 as the baseline, the changes of the mobility are scaled to a baseline as 0, with mobility higher and lower than 0 indicating positive and negative mobility variation, respectively. $Mobility_{i,d}$ refers to the mobility change of the *i*th city on the *d*th day. Specifically, positive and negative values represent the overall increasing and decreasing human activity patterns, with the higher absolute values (regardless of the positive or negative directions) showing the higher-degree activity changes.

The calculated mobility variations for driving and walking transportation in 46 cities are shown in Fig. 6. For the driving transportation, Maricopa in the U.S. reported the highest level of decreasing activities with the value of approximately -0.563, while Pima in the U.S. show the largest increase of driving trips 0.408. It indicates that the proposed policies during COVID-19 yield significant influence on the driving transportation, especially the activity changes during and after the short-term restricted social-distancing policies. For the variation of walking transportation, U.S. Maricopa still reported the highest level of decreasing activities, with the reduction of walking trips of about -0.463. In addition, Alameda in the U.S. reported the largest increase in the walking transportation, with the mobility variation index of approximately 0.357. Those discrepancies of driving and walking transportation among cities are significant for assessing the potential risks of air pollution. For example, the decrease of driving and walking activities in U.S Maricopa could reduce the emission of $PM_{2.5}$, leading to the biases of negative association with daily deaths based on the lag effects of 7, 14 and 21 days.

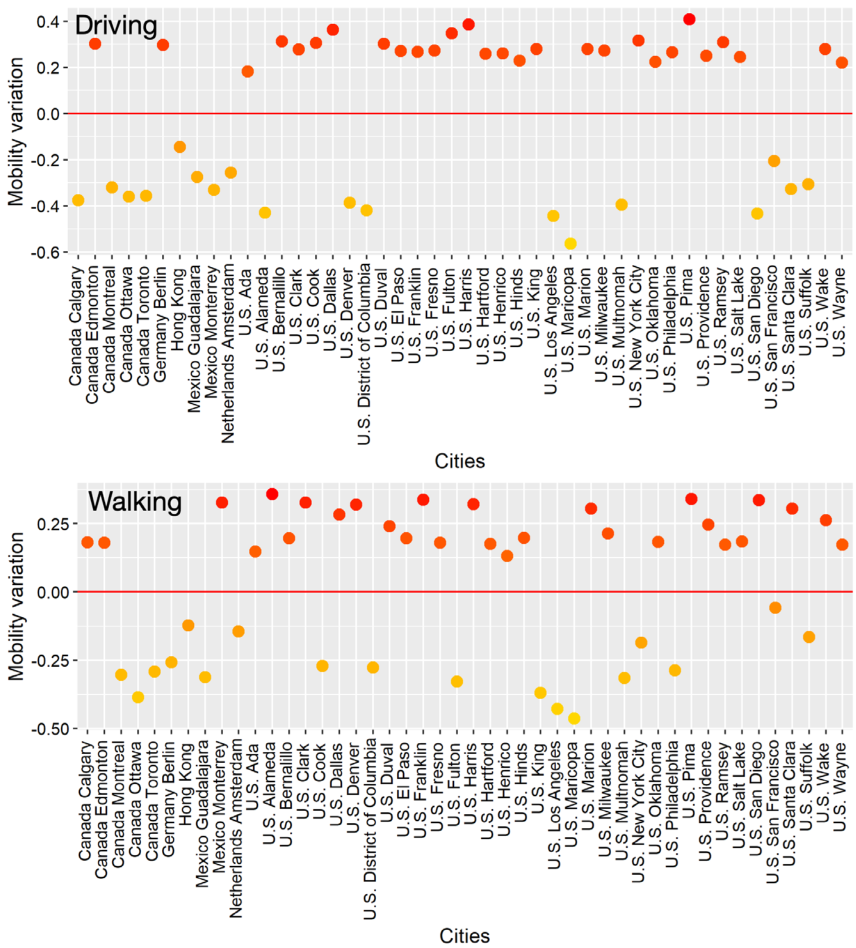

Fig. 6. Mobility variation of driving and walking transportation during 1 Apr. 2020 to 31 Dec. 2020 of individual cities.

In summary, the air pollution - COVID-19 mortality analysis shows discrepancies among individual cities. Influenced by the number of deaths, air pollution conditions and the degree of human mobility variation, biases (usually the negative impact of air pollution) exist in evaluating the relative risks of NO_2 and $PM_{2.5}$ in several cities, such as U.S Henrico, U.S. Pima, Hong Kong, and Canada Calgary. However, the negative trends of relative risks in terms of $PM_{2.5}$ in several cities cannot be explained in this section, such as U.S. Providence and U.S. Wayne, which will be further discussed in the following sections.

Model Assessment

To evaluate the accuracy of BSTHM, comparative studies were proposed by involving GLM and GAM. Specifically, GLM and GAM with negative binomial were utilized to estimate the association between air pollutions with time lag effects (lag 7, lag 14 and lag 21) and COVID-19 mortality. Spatial fixed effects and time fixed effects are included to control spatial and temporal characteristics. For the implement of GAM, the degree of freedom, which is applied for the controlling variables including meteorological and human mobility factors, was selected using the Generalized Cross Validation (GCV) criterion.

The performance of the proposed models, including GLM, GAM and BSTHM, were evaluated by calculating root mean square errors (RMSE). Specifically, RMSE calculates the standard deviation of the prediction error. As shown in Table 4, the RMSE of GLM for the lag 7, lag 14 and lag 21 are 25.181, 21.509, 15.460, respectively. The RMSE of GAM are 24.317, 19.629 and 15.328. For the BSTHM proposed in this study, the RMSE for l the lag 7, lag 14 and lag 21 are 0.703, 0.721 and 0.726, respectively. It indicates that BSTHM achieves better performance than GLM and GAM. However, one should be noted that although lower value of RMSE represents better model performance, it could also lead to over-fitting issue. Since we focus on the overall trends of model regression instead of classification, the biases caused by the potential over-fitting problem could be reduced. On this basis, the overall relative risks of NO_2 and $PM_{2.5}$ were further estimated and compared among GLM, GAM and BSTHM.

Table 4. RMSE calculated from GLM, GAM and STHBM models with different lag effects.

Models	Lag 7	Lag 14	Lag 21
GLM	25.181	21.509	15.460
GAM	24.317	19.629	15.328
BSTHM	0.703	0.721	0.726

Fig. 7 shows the relative risk of NO_2 and $PM_{2.5}$ with 95% credible interval based on GLM, GAM and BSTHM. Generally, overall positive trends are revealed with the lag effects of 7, 14 and 21 days. For the NO_2 – mortality association, the relative risks of 1.008 (CI: 1.008 to 1.015), 1.011 (CI: 1.004 to 1.018) and 1.006 (CI: 0.998 to 1.014) are shown with 7-, 14- and 21-day lag effects using GLM. Utilizing GAM, the relative risks of 1.025 (CI: 1.017 to 1.032), 1.026 (CI: 1.019 to 1.034) and 1.021 (CI: 1.013 to 1.029) are estimated for NO_2 under different time lag effects. The relative risks of BSTHM, as reported in the *Overall BSTHM Results* section, show the values of 1.009 (CI: 1.003 to 1.014), 1.014 (CI: 0.995 to 1.02) and 1.006 (CI: 0.999 to 1.012) under each lag effect scenario. For the $PM_{2.5}$ – mortality association, the relative risks of GLM, GAM and BSTHM are 1.004 (CI: 1.002 to 1.005), 1.001 (CI: 0.999 to 1.003) and 1.002 (CI: 1.001 to 1.003) under the 7-day lag effect, 1.003 (CI: 1.002 to 1.005), 1.001 (CI: 0.999 to 1.003) and 1.002 (CI: 1.001 to 1.003) under the 14-day lag effect, 1.003

(CI: 1.001 to 1.004), 1.001 (CI: 0.999 to 1.003) and 1.004 (1.002 to 1.006) under the 21-day lag effect.

Based on the relative risk estimation in Fig. 7, one can see that different lag effects including 7, 14 and 21 days reveal limited impacts on the relative risk variation. Discrepancies are mainly caused by different models. Compared with GLM and BSTHM, GAM shows higher relative risks of NO_2 with different lag effects. Similar relative risk patterns of NO_2 are revealed using GLM and BSTHM, which are all lower than the relative risks of GAM. For the relative risks of $PM_{2.5}$, lag effects of 7 days and 14 days show similar relative risk patterns, with GLM exhibiting highest risks and GAM yielding lowest risks. Differences are shown in the lag effect of 21 days, with BSTHM reporting the highest risk compared with GAM and GLM. Although discrepancies are found among different models, which are consistent with the model evaluation in Table 4, the overall risk trends based on GLM, GAM and BSTHM are similar, revealing the reliability of the proposed model on the risk estimation.

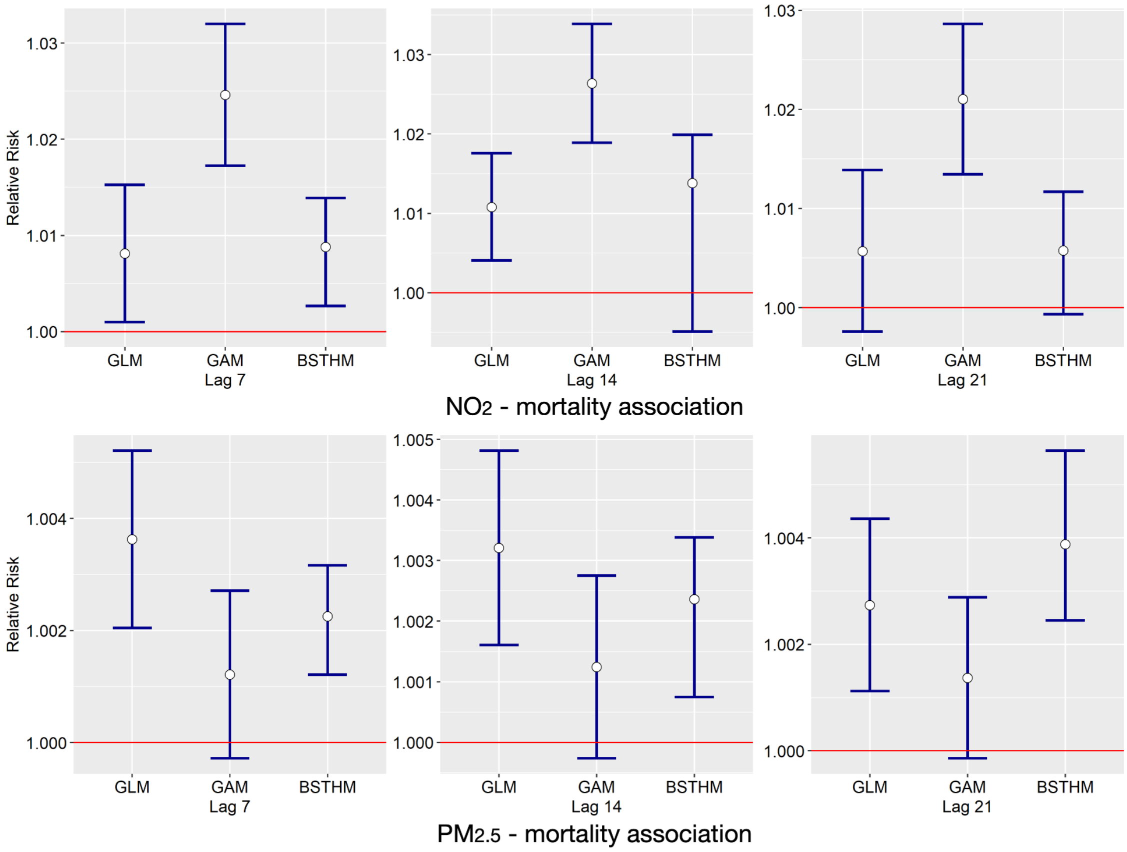

Fig. 7. Relative risk (with 95% credible interval) comparison among GLM, GAM and BSTHM.

Discussion

Although studies of air pollution and epidemic diseases have benefitted from existing research which considers multi-perspective physical and socioeconomic factors (Silva et al. 2017; Srivastava 2020; Rahimi et al. 2020), a better understanding of the local spatial variations of air pollution-COVID-19 interactions has not been well-studied. This study explored the association between daily air pollutants, including NO_2 and $PM_{2.5}$, and COVID-19 mortality between 1 Apr. 2020 and 31 Dec. 2020. The epidemiological analysis focuses on the relative risks of NO_2 and $PM_{2.5}$ to the changes of daily deaths based on a global scale and individual cities.

The results are consistent with the previous studies that higher NO_2 and $PM_{2.5}$ emissions are associated with the increasing deaths caused by respiratory diseases (Xiao et al. 2020; Zoran et al. 2020). Liu et al. (2019) reported the independent association between short-term exposure to $PM_{2.5}$ and daily respiratory diseases in more than 600 cities on a global scale. Moreover, Villeneuve and Goldberg (2020) have provided a literature review on the ambient air pollution and the increasing risk of severe acute respiratory syndrome (SARS) and COVID-19, with all the studies reporting positive associations. In addition, long-term exposure to NO_2 and $PM_{2.5}$ was explored by Zhang et al. (2021), which was positively associated with the increasing risks of respiratory mortality.

It should be noted that despite the positive trends on a global scale, several individual cities in this study, have reported negative association between NO_2, $PM_{2.5}$ and COVID-19 mortality, which is opposite to the overall global trends. The findings reveal the impact of multiple spatial scales on estimating air pollution risks. Previous studies have discussed the influence of multi-scale air pollution on the public health, involving both scales and boundary districts (Thompson and Selin 2012; Markakis et al. 2014). Butt et al. (2017) analyzed the influence of $PM_{2.5}$ in several regions on the changes of global attributable deaths, indicating that the increasing global population weighted $PM_{2.5}$ was mainly dominated by the increase of China and India. Another research by Thompson and Selin (2012) evaluated the uncertainty of air quality and health impacts based on different scales, showing the variation of ozone concentration at 36, 12, 4 and 2 km resolution. Those discrepancies of relative risks have also been discussed in the *City-level Analysis* section of this study. The changes of COVID-19 mortality, the level of air pollution and human mobility variation in individual cities are considered to discuss the relative risk discrepancies. For instance, smaller number of total deaths, lower-level air pollution and higher-level human mobility variation could lead to the biases in relative risk estimation. However, the relative risk patterns in several cities, such as U.S. Providence and Wayne, were not explained by the above factors. It reveals the fact that compared with the classic risk factors, short-term exposure to air pollution shows lower impact on health condition which could lead to the non-positive associations (Liu et al. 2019).

This study has a few new findings. First, it provides evidence on potential risks of air pollution exposure under the scenario of lockdown and restricted social-distancing policies before vaccination. Second, both global and city-level analysis were investigated and compared to illustrate the impact of multi-scale variation on risk estimation of air pollution. This research reinforces the evidence of the discrepancies of linkages between daily NO_2, $PM_{2.5}$ and COVID-19 mortality on the city scale and global scale.

There are also some limitations of this study, i.e., cities selected in this study are limited due to the availability of multi-sourced daily data. For instance, cities which lack ground-level air pollution data are excluded in this study. Air pollution exposure estimation based on the integration of ground-level and satellite-level air pollution data is not considered in this study because of the biases on the fine-scale daily data estimation (Sullivan and Krupnick 2018). Thus, the coverage of the collected data may be not representative to estimate the air pollutants – COVID-19 mortality on a complete global scale. Moreover, although the overall trends of air pollution risks among models have been assessed in the *Model Assessment* section, the discrepancies of relative risks caused by GLM, GAM and BSTHM in individual cities have not been discussed. Evidence about the estimation biases could be provided by comparing individual city-level relative risks of NO_2 and $PM_{2.5}$. For instance, by comparing the relative risks of

$PM_{2.5}$ using GLM and GAM in individual cities, the negative association trends in the U.S. Providence estimated by BSTHM could be further evaluated.

Conclusion

Understanding the association between multi-scale air pollution and COVID-19 mortality is significant in finding the potential factors that could increase the severity of COVID-19 infections. This study provided a global perspective of the ground-level daily NO_2, and $PM_{2.5}$ between 1 Apr. 2020 and 31 Dec. 2020, and estimated multi-scale relative risks of these air pollutants accounting for the meteorological and human mobility factors using a BSTHM model.

Results suggested a significant relationship between daily ground-level air pollutants and COVID-19 mortality based on BSTHM. With the lag effects of 7, 14 and 21 days, the relative risks of NO_2 and $PM_{2.5}$, ranging from 1.006 to 1.014 and from 1.002 to 1.004 respectively, are higher with the increasing number of daily deaths. Moreover, variations of relative risks are shown among individual cities. Relative risks of NO_2 based on 7-, 14- and 21-days' lag effects are between 0.754 and 1.138, between 0.973 and 1.245, and between 0.935 and 1.141, while the relative risks of $PM_{2.5}$ range from 0.888 to 1.032, from 0.968 to 1.013, and from 0.971 to 1.023 with the lag effects of 7, 14 and 21 days. Findings reveal the discrepancies in assessing air pollution in individual cities compared with global analysis, exhibiting the necessity to investigate the potential impact of multi-scale spatial effect of the global air pollution on the COVID-19 mortality.

Acknowledgment

We thank the funding support from grants by the General Research Fund (Grant no. 15603920), the Collaborative Research Fund (Grant no. C7064-18GF) and the Research Institute for

Sustainable Urban Development (Grant no. 1-BBWD), the Hong Kong Polytechnic University, the Hong Kong Research Grants Council (General Research Fund Grant no. 14605920; Collaborative Research Fund Grant no. C4023-20GF), the Research Committee on Research Sustainability of Major Research Grants Council Funding Schemes of the Chinese University of Hong Kong.

References:

Akimoto, H. 2003. Global air quality and pollution. *Science* 302 (5651):1716-1719.

Andrée, B. P. J. 2020. *Incidence of COVID-19 and connections with air pollution exposure: evidence from the Netherlands*: The World Bank.

Barnett-Itzhaki, Z., and A. Levi. 2021. Effects of chronic exposure to ambient air pollutants on COVID-19 morbidity and mortality-A lesson from OECD countries. *Environmental research*:110723.

Bashir, M. F., B. Ma, B. Komal, M. A. Bashir, D. Tan, and M. Bashir. 2020. Correlation between climate indicators and COVID-19 pandemic in New York, USA. *Science of The Total Environment* 728:138835.

Besag, J., J. York, and A. Mollié. 1991. Bayesian image restoration, with two applications in spatial statistics. *Annals of the institute of statistical mathematics* 43 (1):1-20.

Bishop, G., and G. Welch. 2001. An introduction to the kalman filter. *Proc of SIGGRAPH, Course* 8 (27599-23175):41.

Brunekreef, B., and S. T. Holgate. 2002. Air pollution and health. *The Lancet* 360 (9341):1233-1242.

Butt, E., S. Turnock, R. Rigby, C. Reddington, M. Yoshioka, J. Johnson, L. Regayre, K. Pringle, G. Mann, and D. Spracklen. 2017. Global and regional trends in particulate air pollution and attributable health burden over the past 50 years. *Environmental Research Letters* 12 (10):104017.

Chang, S., E. Pierson, P. W. Koh, J. Gerardin, B. Redbird, D. Grusky, and J. Leskovec. 2021. Mobility network models of COVID-19 explain inequities and inform reopening. *Nature* 589 (7840):82-87.

Chen, R., H. Kan, B. Chen, W. Huang, Z. Bai, G. Song, and G. Pan. 2012. Association of particulate air pollution with daily mortality: the China Air Pollution and Health Effects Study. *American journal of epidemiology* 175 (11):1173-1181.

Chinazzi, M., J. T. Davis, M. Ajelli, C. Gioannini, M. Litvinova, S. Merler, A. P. y Piontti, K. Mu, L. Rossi, and K. Sun. 2020. The effect of travel restrictions on the spread of the 2019 novel coronavirus (COVID-19) outbreak. *Science* 368 (6489):395-400.

Chowkwanyun, M., and A. L. Reed Jr. 2020. Racial health disparities and Covid-19—caution and context. *New England Journal of Medicine* 383 (3):201-203.

Chu, D. K., E. A. Akl, S. Duda, K. Solo, S. Yaacoub, H. J. Schünemann, A. El-harakeh, A. Bognanni, T. Lotfi, and M. Loeb. 2020. Physical distancing, face masks, and eye protection to prevent person-to-person transmission of SARS-CoV-2 and COVID-19: a systematic review and meta-analysis. *The Lancet* 395 (10242):1973-1987.

Coccia, M. 2020. Factors determining the diffusion of COVID-19 and suggested strategy to prevent future accelerated viral infectivity similar to COVID. *Science of The Total Environment*:138474.

———. 2021. The effects of atmospheric stability with low wind speed and of air pollution on the accelerated transmission dynamics of COVID-19. *International Journal of Environmental Studies* 78 (1):1-27.

Di, Q., L. Dai, Y. Wang, A. Zanobetti, C. Choirat, J. D. Schwartz, and F. Dominici. 2017. Association of short-term exposure to air pollution with mortality in older adults. *Jama* 318 (24):2446-2456.

Dunson, D. B. 2001. Commentary: practical advantages of Bayesian analysis of epidemiologic data. *American journal of epidemiology* 153 (12):1222-1226.

Forster, P. M., H. I. Forster, M. J. Evans, M. J. Gidden, C. D. Jones, C. A. Keller, R. D. Lamboll, C. Le Quéré, J. Rogelj, and D. Rosen. 2020. Current and future global climate impacts resulting from COVID-19. *Nature Climate Change* 10 (10):913-919.

Giani, P., S. Castruccio, A. Anav, D. Howard, W. Hu, and P. Crippa. 2020. Short-term and long-term health impacts of air pollution reductions from COVID-19 lockdowns in China and Europe: a modelling study. *The Lancet Planetary Health* 4 (10):e474-e482.

Gujral, H., and A. Sinha. 2021. Association between exposure to airborne pollutants and COVID-19 in Los Angeles, United States with ensemble-based dynamic emission model. *Environmental research* 194:110704.

He, G., Y. Pan, and T. Tanaka. 2020. The short-term impacts of COVID-19 lockdown on urban air pollution in China. *Nature Sustainability* 3 (12):1005-1011.

He, K., H. Huo, and Q. Zhang. 2002. Urban air pollution in China: current status, characteristics, and progress. *Annual review of energy and the environment* 27 (1):397-431.

Khomenko, S., M. Cirach, E. Pereira-Barboza, N. Mueller, J. Barrera-Gómez, D. Rojas-Rueda, K. de Hoogh, G. Hoek, and M. Nieuwenhuijsen. 2021. Premature mortality due to air pollution in European cities: a health impact assessment. *The Lancet Planetary Health* 5 (3):e121-e134.

Knorr-Held, L. 2000. Bayesian modelling of inseparable space-time variation in disease risk. *Statistics in medicine* 19 (17-18):2555-2567.

Kwok, C. Y. T., M. S. Wong, K. L. Chan, M.-P. Kwan, J. E. Nichol, C. H. Liu, J. Y. H. Wong, A. K. C. Wai, L. W. C. Chan, and Y. Xu. 2021. Spatial analysis of the impact of urban geometry and socio-demographic characteristics on COVID-19, a study in Hong Kong. *Science of The Total Environment* 764:144455.

Le Quéré, C., R. B. Jackson, M. W. Jones, A. J. Smith, S. Abernethy, R. M. Andrew, A. J. De-Gol, D. R. Willis, Y. Shan, and J. G. Canadell. 2020. Temporary reduction in daily global CO 2 emissions during the COVID-19 forced confinement. *Nature Climate Change* 10 (7):647-653.

Lelieveld, J., J. S. Evans, M. Fnais, D. Giannadaki, and A. Pozzer. 2015. The contribution of outdoor air pollution sources to premature mortality on a global scale. *Nature* 525 (7569):367-371.

Li, J., J. Wang, N. Wang, and H. Li. 2018a. A Bayesian space–time hierarchical model for remotely sensed lattice data based on multiscale homogeneous statistical units. *IEEE Journal of Selected Topics in Applied Earth Observations and Remote Sensing* 11 (7):2151-2161.

Li, J., N. Wang, J. Wang, and H. Li. 2018b. Spatiotemporal evolution of the remotely sensed global continental PM2. 5 concentration from 2000-2014 based on Bayesian statistics. *Environmental pollution* 238:471-481.

Li, S., S. Ma, and J. Zhang. 2021. Association of built environment attributes with the spread of COVID-19 at its initial stage in China. *Sustainable cities and society*:102752.

Liao, J., Z. Qin, Z. Zuo, S. Yu, and J. Zhang. 2016. Spatial-temporal mapping of hand foot and mouth disease and the long-term effects associated with climate and socio-economic variables in Sichuan Province, China from 2009 to 2013. *Science of The Total Environment* 563:152-159.

Liu, C., R. Chen, F. Sera, A. M. Vicedo-Cabrera, Y. Guo, S. Tong, M. S. Coelho, P. H. Saldiva, E. Lavigne, and P. Matus. 2019. Ambient particulate air pollution and daily mortality in 652 cities. *New England Journal of Medicine* 381 (8):705-715.

Ma, Y., Y. Zhao, J. Liu, X. He, B. Wang, S. Fu, J. Yan, J. Niu, J. Zhou, and B. Luo. 2020. Effects of temperature variation and humidity on the death of COVID-19 in Wuhan, China. *Science of The Total Environment* 724:138226.

Markakis, K., M. Valari, A. Colette, O. Sanchez, O. Perrussel, C. Honore, R. Vautard, Z. Klimont, and S. Rao. 2014. Air quality in the mid-21st century for the city of Paris under two climate scenarios; from the regional to local scale. *Atmospheric Chemistry and Physics* 14 (14):7323-7340.

Mathieu, E., H. Ritchie, E. Ortiz-Ospina, M. Roser, J. Hasell, C. Appel, C. Giattino, and L. Rodés-Guirao. 2021. A global database of COVID-19 vaccinations. *Nature human behaviour*:1-7.

Meng, Y., M. S. Wong, H. Xing, R. Zhu, K. Qin, M.-P. Kwan, K. H. Lee, C. Y. T. Kwok, and H. Li. 2021. Effects of urban functional fragmentation on nitrogen dioxide (NO2) variation with anthropogenic-emission restriction in China. *Scientific reports* 11 (1):1-15.

Ming, W., Z. Zhou, H. Ai, H. Bi, and Y. Zhong. 2020. COVID-19 and air quality: Evidence from China. *Emerging Markets Finance and Trade* 56 (10):2422-2442.

Ogen, Y. 2020. Assessing nitrogen dioxide (NO2) levels as a contributing factor to the coronavirus (COVID-19) fatality rate. *Science of The Total Environment*:138605.

Prata, D. N., W. Rodrigues, and P. H. Bermejo. 2020. Temperature significantly changes COVID-19 transmission in (sub) tropical cities of Brazil. *Science of The Total Environment* 729:138862.

Rahimi, N. R., R. Fouladi-Fard, R. Aali, A. Shahryari, M. Rezaali, Y. Ghafouri, M. R. Ghalhari, M. A. Ghalhari, B. Farzinnia, and M. Fiore. 2020. Bidirectional Association Between COVID-19 and the Environment: a Systematic Review. *Environmental research*:110692.

Richardson, S., J. J. Abellan, and N. Best. 2006. Bayesian spatio-temporal analysis of joint patterns of male and female lung cancer risks in Yorkshire (UK). *Statistical methods in medical research* 15 (4):385-407.

Sarkodie, S. A., and P. A. Owusu. 2020. Impact of meteorological factors on COVID-19 pandemic: Evidence from top 20 countries with confirmed cases. *Environmental research* 191:110101.

Shan, Y., J. Ou, D. Wang, Z. Zeng, S. Zhang, D. Guan, and K. Hubacek. 2020. Impacts of COVID-19 and fiscal stimuli on global emissions and the Paris Agreement. *Nature Climate Change*:1-7.

Shao, W., J. Xie, and Y. Zhu. 2021. Mediation by human mobility of the association between temperature and COVID-19 transmission rate. *Environmental research* 194:110608.

Silva, R. A., J. J. West, J.-F. Lamarque, D. T. Shindell, W. J. Collins, G. Faluvegi, G. A. Folberth, L. W. Horowitz, T. Nagashima, and V. Naik. 2017. Future global mortality from changes in air pollution attributable to climate change. *Nature Climate Change* 7 (9):647-651.

Srivastava, A. 2020. COVID-19 and air pollution and meteorology-an intricate relationship: A review. *Chemosphere*:128297.

Sullivan, D. M., and A. Krupnick. 2018. Using satellite data to fill the gaps in the US air pollution monitoring network. *Resources for the Future Working Paper*:18-21.

Thompson, T. M., and N. E. Selin. 2012. Influence of air quality model resolution on uncertainty associated with health impacts. *Atmospheric Chemistry and Physics* 12 (20):9753-9762.

Travaglio, M., Y. Yu, R. Popovic, L. Selley, N. S. Leal, and L. M. Martins. 2021. Links between air pollution and COVID-19 in England. *Environmental pollution* 268:115859.

Venter, Z. S., K. Aunan, S. Chowdhury, and J. Lelieveld. 2020. COVID-19 lockdowns cause global air pollution declines. *Proceedings of the National academy of Sciences* 117 (32):18984-18990.

Villeneuve, P. J., and M. S. Goldberg. 2020. Methodological considerations for epidemiological studies of air pollution and the SARS and COVID-19 coronavirus outbreaks. *Environmental health perspectives* 128 (9):095001.

Wang, Z., Y. Yue, B. He, K. Nie, W. Tu, Q. Du, and Q. Li. 2021. A Bayesian spatio-temporal model to analyzing the stability of patterns of population distribution in an urban space using mobile phone data. *International Journal of Geographical Information Science* 35 (1):116-134.

Weiss, D., A. Nelson, C. Vargas-Ruiz, K. Gligorić, S. Bavadekar, E. Gabrilovich, A. Bertozzi-Villa, J. Rozier, H. Gibson, and T. Shekel. 2020. Global maps of travel time to healthcare facilities. *Nature Medicine* 26 (12):1835-1838.

Xiao, W., R. Nethery, B. Sabath, D. Braun, and F. Dominici. 2020. Exposure to air pollution and COVID-19 mortality in the United States. *medRxiv*.

Xie, J., and Y. Zhu. 2020. Association between ambient temperature and COVID-19 infection in 122 cities from China. *Science of The Total Environment* 724:138201.

Yancy, C. W. 2020. COVID-19 and african americans. *Jama* 323 (19):1891-1892.

Zhang, Z., J. Wang, J. C. Kwong, R. T. Burnett, A. van Donkelaar, P. Hystad, R. V. Martin, L. Bai, J. McLaughlin, and H. Chen. 2021. Long-term exposure to air pollution and mortality in a prospective cohort: The Ontario Health Study. *Environment international* 154:106570.

Zhu, Y., J. Xie, F. Huang, and L. Cao. 2020a. Association between short-term exposure to air pollution and COVID-19 infection: Evidence from China. *Science of The Total Environment*:138704.

Zhu, Y., J. Xie, F. Huang, and L. Cao. 2020b. The mediating effect of air quality on the association between human mobility and COVID-19 infection in China. *Environmental research* 189:109911.

Zoran, M. A., R. S. Savastru, D. M. Savastru, and M. N. Tautan. 2020. Assessing the relationship between surface levels of PM2. 5 and PM10 particulate matter impact on COVID-19 in Milan, Italy. *Science of The Total Environment* 738:139825.